**INTERNATIONAL JOURNAL OF OPTIMIZATION IN CIVIL ENGINEERING**
***Int. J. Optim. Civil Eng., 2020; 10(3):513-529***

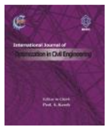

# WEIGHT MINIMIZATION AND ENERGY DISSIPATION MAXIMIZATION OF BRACED FRAMES USING EVPS ALGORITHM

A. Kaveh[1*, †], S. R. Hoseini Vaez[2], P. Hosseini[3] and H. Abedini[2]
*[1]Centre of Excellence for Fundamental Studies in Structural Engineering, School of Civil Engineering, Iran University of Science and Technology, Narmak, Tehran-16, Iran*
*[2]Department of Civil Engineering, Faculty of Engineering, University of Qom, Qom*
*[3]Faculty of Engineering, Mahallat Institute of Higher Education, Mahallat, Iran*

## ABSTRACT

In this research, a new objective function has been proposed for optimal design of the Buckling Restrained Braced Frames (BRBFs) is performed using nonlinear time history analysis. The BRBF is a particular type of bracing system that has been widely utilized in recent years. The nonlinear time history analysis also provides a detailed view of the behavior of the structure. The purpose of this study is to provide an optimal design based on minimizing the weight of the structure while increasing the energy dissipation capability of the structure. Due to the complexity of the problem, the Enhanced Vibrating Particles Systems (EVPS) meta-heuristic algorithm is used to perform the optimization. Here, a 3-story frame, a 6-story frame and a 9-story frame are investigated simultaneously considering the continuous and discrete optimization.

**Keywords:** buckling restrained braced frames, weight optimization, enhanced vibrating particles systems algorithm, structural optimization.

Received: 20 March 2020; Accepted: 10 July 2020

## 1. INTRODUCTION

The use of meta-heuristic algorithms has been widespread over the years. These types of optimization techniques are approximate methods that provide a reasonable answer in a manageable time. The use of these methods has been successfully explored in many civil

[*]Corresponding author: School of Civil Engineering, Iran University of Science and Technology, Narmak, Tehran-16, Iran
[†]E-mail address: alikaveh@iust.ac.ir (A. Kaveh)

and structural engineering publications [1-8]. It should be noted that new meta-heuristic algorithms are being introduced nowadays that outperform previous methods in speed or accuracy as well as used in specific problems. Many meta-heuristic algorithms are presented in the last two decades, some of them are listed as follows:

Differential Evolution (DE) [9], Particle Swarm Optimization (PSO) [10], Colliding Bodies Optimization (CBO) and Enhanced Colliding Bodies Optimization (ECBO) [11], Binary artificial algae algorithm [12], Electro-Search algorithm [13], Thermal exchange optimization [14] and Vibrating particle algorithm (VPS) [15].

The EVPS algorithm is an enhanced version of the VPS algorithm, Kaveh et al. [16]. This algorithm is adopted from the free vibration of single degree of freedom systems with viscous damping. The enhanced version uses some new mechanisms to promote the performance of the VPS algorithm. These mechanisms are employed to improve the ability of the standard VPS to perform a global search and prevent entrapment in local optima [17].

Buckling Restrained Braced Frames (BRBF) system is a particular type of bracing system that has recently been extensively used. The BRBF consists of a ductile steel core that exhibits suitable comparison and tension behavior. The steel core, which is enclosed in a steel sheath, is filled with concrete, thus preventing the buckling of these sections.

The use of nonlinear time history analysis improves the accuracy of structural analysis and it is a more realistic method of analysis. This method has been extensively used in optimal design of structures in recent years [18-26].

Optimizing the cross-sectional area of the buckling restrained braces not only reduces the cost of fabricating also provides more realistic results by using nonlinear time history analysis.

Finite element (FE) models of steel BRBs with varied geometries were subjected to cyclic analyses and the satisfactory brace geometries that minimized instability of the core section while maximizing energy dissipation capacity were identified by Hosseinzadeh and Mohebi in 2016 [27]. A novel self-centering buckling restrained brace (SC-BRB) developed and applied to reinforced concrete double-column bridge pier for seismic retrofitting by Dong et al. in 2017 [28]. Sabelli et al. [29] investigated the seismic response of three and six-story concentrically braced frames utilizing buckling-restrained braces. Kiggins and Uang [30] in 2006 evaluated the potential benefit of using buckling-restrained braces in a dual system to minimize permanent deformations. A formulation for optimum yield strength of BRB that maximizes the equivalent damping ratio was derived and nonlinear dynamic time-history analyses were carried out to investigate the seismic response of model structures with BRB by Kim and Choi [31]. Sahoo and Chao presented a performance-based plastic design (PBPD) methodology for the design of buckling-restrained braced frames (BRBFs) in 2010 [32]. Miller et al. presented a viable solution including experimental investigation of the cyclic behavior and performance of a self-centering buckling-restrained brace (SC-BRB), the SC-BRB they researched, consists of a typical BRB component, which provides energy dissipation, and pre-tensioned superelastic nickel-titanium (NiTi) shape memory alloy (SMA) rods, which provide self-centering and additional energy dissipation [33]. Hoveidae and Rafezy developed a finite element analysis for all-steel buckling restrained braces that have identical core sections, but different buckling restraining mechanisms and the objective of the analysis is to conduct a parametric study of BRBs with different amounts of a gap and initial imperfections to investigate the global buckling behavior of the brace [34]. Experimental Evaluation of a Large-Scale Buckling-Restrained Braced Frame is performed by Fahnestock in 2007 [35]. Seismic Response and Performance of Buckling-Restrained Braced Frames was conducted also describes the nonlinear dynamic analyses that were performed by Fahnestock [36].

Abedini et al. [37] optimized two problems consisting of three-story and six-story frames. They used a two-term objective function, which was normalized with estimated constant values to optimize the problems. The objective function presented in the mentioned research may get trapped in local optima.

Ductility and high-energy dissipation in this type of braces along with their resistance against buckling, make them different from other lateral force resisting systems. Massive inelastic deformation resistance results in high-energy absorption and at this phase as much as the structure bears large deformation, it absorbs more energy. Thus as much as the ability of energy absorption increases, the structure absorbs less energy from earthquakes. So it is highly regarded to use buckling restrained braces which cause increasing ductility (plasticity) and decreasing demand for structure for lateral forces resistance.

Applying metaheuristic algorithms is appropriate for the optimum design of these structures using time history analysis. Because these types of problems have many complicated parameters and constraints. This paper investigates to apply EVPS metaheuristic algorithms and nonlinear time history analysis for optimum design of buckling restrained braces. The purpose of optimization in this research is to minimize the weight of structure with the utmost energy dissipation. Braces are placed in chevron arrangement which is common in buckling restrained braces. It should be noted that the section of beams is constantly given in the optimization process.

In this study, a new objective function is proposed for solving these types of problems, which normalized using dynamic parameters. So, this attempt has been made to provide an objective function with more capabilities to escape from the local optima. The results of the new objective function are compared with the results of the previous research. The presented results clearly show the capabilities of the proposed objective function to escape the local optima. In addition, a larger and more complex problem has been investigated. It should be mentioned that all the problems of this study have been studied with the EVPS algorithm and their results have been compared with Abedini et al. [37] research. For solving the new problem, two EVPS and ECBO algorithms are used. Also, one more earthquake ground motion record is utilized for comparison with the mentioned research [37].

This paper is organized as follow:

After this introductory section, a brief explanation of nonlinear time history analysis and the selected record is presented in section 2. The optimal design of structures with BRBFs (consisting of formulations of the objective function and the constraints of this study) is provided in section 3. In section 4, a brief explanation of the EVPS algorithm is presented. Section 5 presents the numerical problems that include two BRB frames. Concluding is provided in the last section.

## 2. NONLINEAR TIME HISTORY ANALYSIS

Regardless of the approximate assumptions about strain hardening, it is possible to calculate the exact amount of strain demand for buckling restrained braced Frames using nonlinear time history analysis. Using this type of analysis, it is also possible to directly evaluate the structural response and the cumulative ductility demand of BRBs [38]. Therefore, the Newmark average acceleration method with Newton-Raphson iteration was used for time history analysis.

In this study, four earthquake ground motion records with the characteristics presented in Table 1 are used. These records were selected from a site in Los Angeles, California that were compiled using the ASCE (2013) acceleration spectrum and were scaled to the level of seismic hazard with a 10% probability of exceedance in 50 years [39]. Fig. 1 shows the acceleration spectrum of the records. OpenSees was used for nonlinear time history analysis [40].

Table 1: Characteristics and accelerometer scale factors

| Record | Earthquake event | Year | PGA ($m/s^2$) | Scale factor |
|---|---|---|---|---|
| LA01 | Imperial Valley El Centro | 1940 | 4.52 | 2.01 |
| LA12 | Loma Prieta Gilory | 1989 | 9.5 | 1.79 |
| LA14 | Northridge Newhal | 1994 | 6.44 | 1.03 |
| LA16 | Northridge RinaldiRS | 1994 | 5.68 | 0.79 |

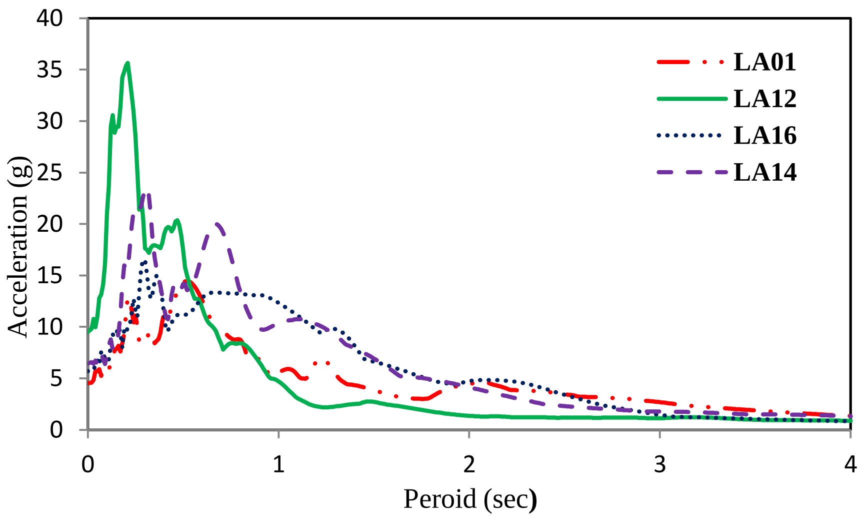


Figure 1. Spectrum acceleration of the records

## 3. OPTIMAL DESIGN OF STRUCTURES WITH BRBFS

An optimization problem is generally presented in Eq. (1). The purpose of this equation is to minimize the objective function provided that the constraints of the optimization problem are met.

$$\begin{aligned} & Minimize \;\; f(x) \\ & Subjected\ to \begin{cases} g_i(x) \leq 0 & i = 1, 2, \ldots, p \\ h_i(x) = 0 & j = 1, 2, \ldots, m \\ L_k \leq X_k \leq U_k & k = 1, 2, \ldots, n \end{cases} \end{aligned} \tag{1}$$

where $f$(x) is the objective function and $g_i$(x) and $h_i$(x) are the inequality and equality constraints of the optimization problem, respectively.

### *3.1 Objective function*

The selection of a proper objective function is an important step toward optimization. In some cases, the problem will require multi-objective optimization, which means that several objective functions will have to be minimized. One of the simplest solutions is to define a new objective function based on the linear combination of each objective function in multi-objective optimization. In this study, the objective function has two purposes consisting of normalized functions $F_1$ and $F_2$ according to Eq. (2).

$$f(X) = F_1 + F_2 \tag{2}$$

where $F_1$ and $F_2$ represent the weight and the amount of energy dissipation, respectively. $F_1$ is the normalized weight of the structure function obtained using Eq. (3). $F_2$ will be introduced in the following. The column sections have been selected from the list of American sections [41] and the cross-sectional area of the braces is assumed to vary from 0.0005 to 0.02024 m$^2$.

$$F_1 = \frac{\sum_{i=1}^{ne} (\rho_i A_i L_i)}{W_{optimum}} \tag{3}$$

where $\rho$ , $L_i$ , $A_g$ are the density of steel, the length and area of the $i^{th}$ element, *ne* is the total number of structural elements. $W_{optimum}$ parameter is given a hypothetical value in the first run and from the second run, this parameter equals the best weight of the best answer that obtained until that run.

The $F_2$ function denotes the normalized energy dissipation calculated according to the Eq. (4). Structural energy depreciation is an essential parameter in evaluating the performance of the structure. Also, it can be used as a measurement of its ductility in the plastic zone. The higher area under the hysteresis subsurface means more energy dissipation of the structure and the greater the ductility of the structure. In the following, there are some of the constraints that intended for this study. By providing these constraints, it can be shown that an increase in dissipated energy leads to a better performance of the structure.

$$F_2 = \frac{AR_{optimum}}{AR} \tag{4}$$

where $AR_{optimum}$ parameter is given a hypothetical value in the first run and from the second run, this parameter equals the best energy dissipation of the best answer that obtained until that run. *AR* is the ratio of the total area under the hysteresis curve to the area under the elastic zone and is calculated as the following equation:

$$AR = \sum_{i=1}^{n_s} \frac{Area_i}{(Area_i)_y} \tag{5}$$

where $n_s$ is the total number of stories, $Area_i$ is the area under the hysteresis curve of the $i^{th}$ story and $(Area_i)_y$ is the area under the elastic part, which is determined as:

$$(Area_i)_y = 0.5 d_y F_y A_g (X_g) \cos^2 \theta \tag{6}$$

where $d_y$ is the length of the elastic part, $F_y$ is the yield stress of the brace and $\theta$ is the angle of the brace relative to the horizon.

### *3.2 Optimization constraints*

The optimization constraints of this study are summarized as follows:

#### *3.2.1 Deformation constraints*

The relative displacement of the stories is a criterion for evaluating the performance of the structure and is consistent with the results of previous studies [42]. According to ASCE (2010) [43], the maximum relative displacement of stories in structures with up to five stories should not exceed $\Delta_a = 0.025h$ and for other structures should not exceed $\Delta_a = 0.02h$, where $h$ is the total height of the structure.

$$\frac{\Delta_{\max}}{\Delta_a} - 1 \le 0 \tag{7}$$

#### *3.2.3 Strength constraints*

All force-controlled members of the braced frames (columns and beams) should be designed for the expected axial force [44]. States that the ultimate axial load of the columns in compression and tension under LRFD loading should be less than or equal to their nominal axial strength as:

$$P_u \le \phi_c P_n \tag{8}$$

where $\phi_c$ is the strength reduction factor and is equal to 0.9 in compression and tension. $P_u$ is the axial load capacity required under LRFD loading conditions and is calculated as:

$$P_u = 1.2D + 1.0L + 2.5E \tag{9}$$

$P_n$ denotes the nominal strength of the column in compression and tension and is determined as:

$$\begin{gathered} P_n = A_g F_y \\ P_n = F_{cr} A_g \end{gathered} \tag{10}$$

where $A_g$ is the cross-sectional area of the member, $F_y$ is the yield stress of the steel, and $F_{cr}$ is the buckling stress.

*3.2.4 Geometrical constraints*

Limitations on the beam-to-column connections should be considered during optimization to eliminate the design of connections with special configurations. Because the beam sections were assumed to remain unchanged in this study, column sections for which the width of the flange $(b_f)_c$ is less than that of the beam $(b_f)_b$ were omitted from the list of the available sections. The following geometrical constraints were considered:

$$\begin{aligned} &\frac{(d\_col_{s+1})_i}{(d\_col_s)_i} - 1 \le 0 \qquad (i = 1, 2, \ldots, n_{cc}; \qquad s = 1, 2, \ldots, n_s - 1) \\ &\frac{(A\_brb_{s+1})_j}{(A\_brb_s)\, j} - 1 \le 0 \qquad (j = 1, 2, \ldots, n_{brb}; \qquad s = 1, 2, \ldots, n_s - 1) \end{aligned} \tag{11}$$

where $(d\_col_s)_i$ and $(d\_col_{s+1})_i$ are the depth of the $s^{\text{th}}$ and $(s+1)^{\text{th}}$ story columns connected to the $i^{\text{th}}$ column, respectively, and $(A\_brb_s)_j$ and $(A\_brb_{s+1})_j$ are the cross-sectional areas of the brace of the $s^{\text{th}}$ and $(s+1)^{\text{th}}$ stories, respectively. Furthermore, $n_{cc}$, $n_{brb}$, and $n_s$ are the number of column-to-column connections, BRB connections, and stories, respectively.

## 5. OPTIMIZATION ALGORITHM

In this part, Enhanced Vibrating Particles System (EVPS) is briefly presented. The EVPS is a modified version of the VPS algorithm that was presented by Kaveh et al. in 2018 [16, 17]. These modifications result in increasing the convergence speed, augmenting the ability of search, helping the EVPS to escape from local optima and overall resulting in better results. In this method, *Memory* parameter replaced with *HB* parameter of the VPS algorithm. *Memory* parameter saves *Memorysize* number of the best historically positions from the whole population. When the best answer of each *iteration* is better than the worst value of the *Memory,* it should replace the worst value in the *Memory*. Also, in the EVPS algorithm, the equations for generating of the population for next iteration have been changed.

This algorithm has been used to solve various optimization problems [45-46].

## 5. NUMERICAL PROBLEMS

In order to simultaneously optimize the weight and dissipated energy of sample structures consisting of three-story, six-story and nine-story frames depicted in Fig. 2 (including the geometry, grouping of members, and gravity loads for both structures), the EVPS algorithm is used. The population size and numbers of iterations are 30,500 (for the first problem) and 30,300 (for second and third problems), respectively. It should be noted that p, $w_1$, $w_2$, HMCR, PAR and *Memorysize* parameters are 0.2, 0.3, 0.3, 0.95, 0.1 and 4 for all problems. Also, the number of independent runs for each problem is considered 30 times. The yield stress of the steel used for the columns and BRBs was 345 and 248 MPa, respectively. The modulus of elasticity of the steel used for all structural elements was $2.1 \times 10^5$ MPa. The value of $W_1$ and $W_2$ are equal to 21.37 kN/m and 19.84 kN/m, respectively.

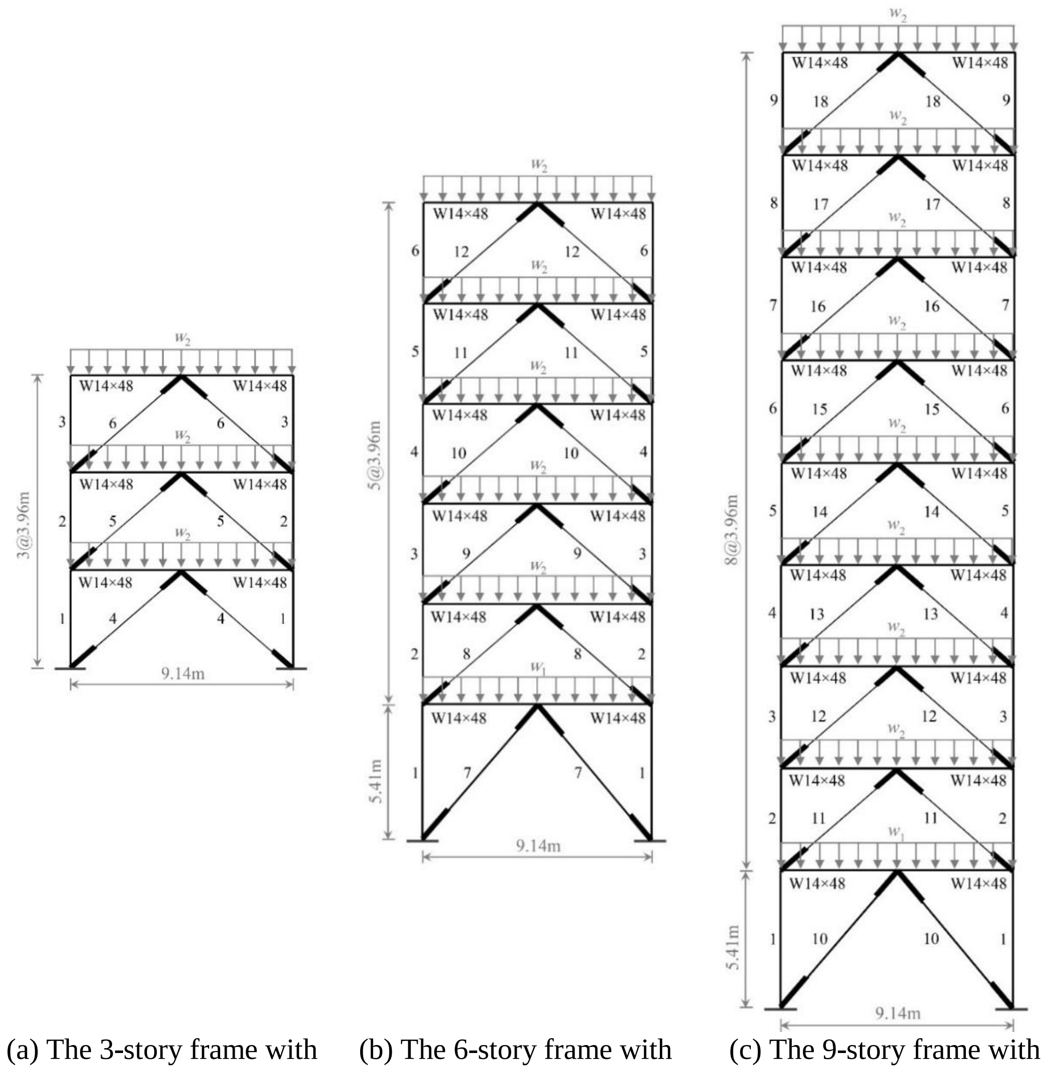


(a) The 3-story frame with BRB (b) The 6-story frame with BRB (c) The 9-story frame with BRB

Figure 2. Geometry, the grouping of members and gravity loading for sample frames

*5.1 One-bay three-story frame*

In this problem, the 3-storey braced frame with BRB is shown in Fig. 2.a. The variation of the *f* (Eq. (2)) against the iteration of the EVPS algorithm for the best answer is illustrated in Fig. 3. Also, this figure shows the trend of decreasing the normalized weight of the structure and increasing normalized energy dissipation for the best solution. Fig. 4 presents the weight, ratio of the area under the hysteresis curve to the area of the elastic zone, and also, the hysteresis curve shows the decrease in base shear (kN) after 5, 25 and 500 iterations which confirms the validity of the optimization.

The optimal sections and the weight of the structures for the best answer gained by EVPS is presented in Table 2. For considering the constraints of the problem consisting of the stress ratio of elements and drift of each story, Fig. 5 is presented.

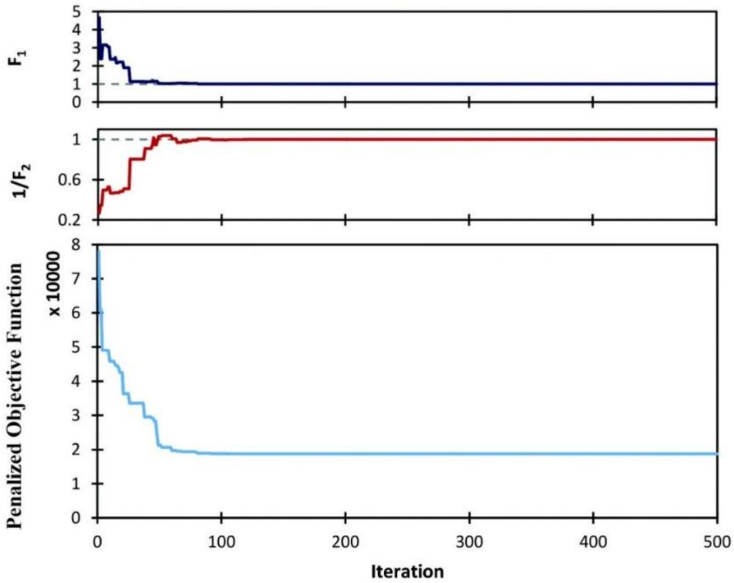


Figure 3. Convergence curve of optimal design of one-bay three-story frame

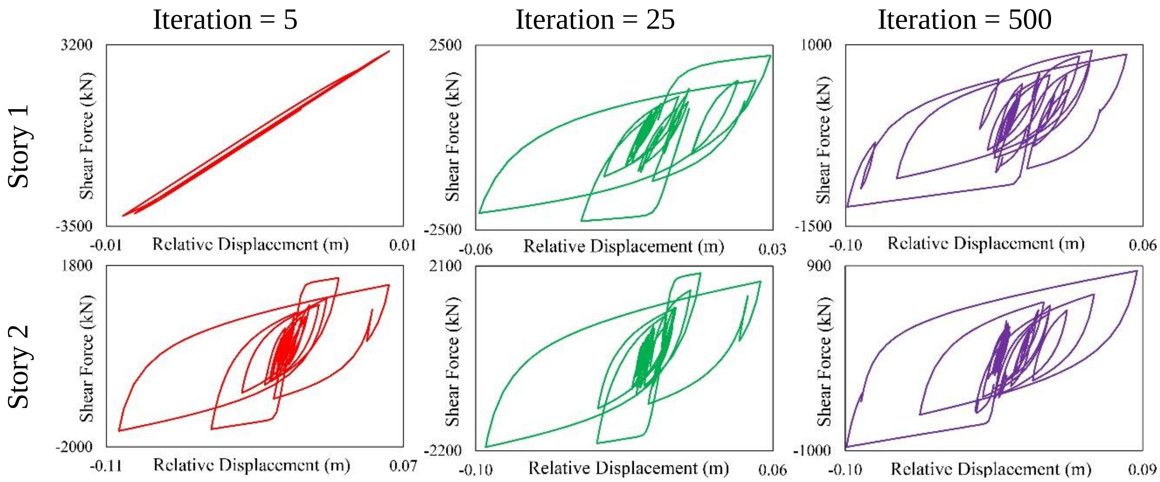

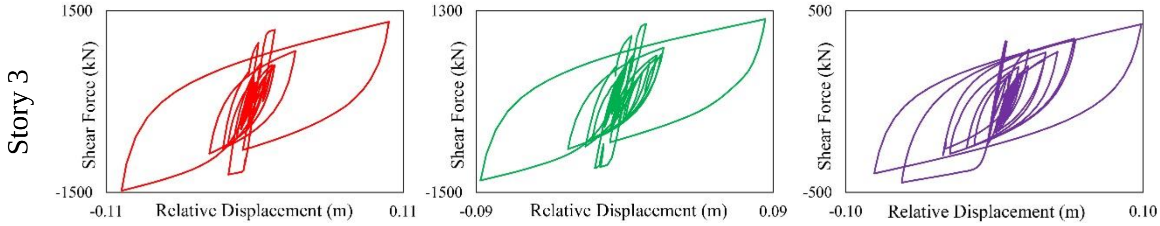


AR=657.64 AR=673.53 AR=1325.22

Weight (kN)=62.103 Weight (kN)=37.419 Weight (kN)=19.727

Figure 4. The hysteresis curve after 5, 25 and 500 iterations for the one-bay three-story frame

Table 2: Properties of optimized sections for sample 1

| **Element group** | **LA01** | | | **LA12** | | | **LA16** | | | **LA14** |
|---|---|---|---|---|---|---|---|---|---|---|
| | **ECBO[37]]** | **SSA[37]]** | **EVPS*** | **ECBO[37]]** | **SSA[37]]** | **EVPS*** | **ECBO[37]]** | **SSA[37]]** | **EVPS*** | **EVPS*** |
| **1** | W24×68 | W27×368 | W44X290 | W21×48 | W18×76 | W44X262 | W30×99 | W36×150 | W40X593 | W44×290 |
| **2** | W12×45 | W27×368 | W44X290 | W12×45 | W12×96 | W44X335 | W12×45 | W24×176 | W40X593 | W40×593 |
| **3** | W10×54 | W21×147 | W44X335 | W8×40 | W8×40 | W44X335 | W8×40 | W8×67 | W44X335 | W40×593 |
| **Columns weight (*kN*)** | 19.281 | 101.99 | 14.913 | 15.307 | 24.475 | 14.76 | 21.209 | 45.487 | 15.7 | 16.25 |
| **4**($mm^2$) | 1879 | 1381 | 1830.641 | 3054 | 500 | 794.9278 | 5713 | 8176 | 1562.412 | 2435 |
| **5**($mm^2$) | 1077 | 668 | 1485.915 | 1894 | 500 | 609.3637 | 5656 | 4076 | 1562.412 | 1912 |
| **6**($mm^2$) | 1077 | 595 | 879.3758 | 500 | 500 | 500 | 2967 | 3249 | 872.8663 | 988 |
| **BRB weight (*kN*)** | 2.6 | 1.723 | 2.73 | 3.55 | 0.977 | 1.24 | 9.3405 | 10.099 | 2.6 | 3.47 |
| **Total weight (*kN*)** | 21.908 | 103.714 | 17.6468 | 18.856 | 25.452 | 15.99642 | 30.549 | 55.586 | 18.30463 | 19.727 |
| **AR** | 1520.45 | 1810.9 | 1900.823 | 994.4 | 1124.9 | 1346.287 | 457.5 | 4118.8 | 1150.435 | 1325.22 |

*** The marked items are obtained using the new objective function (Eq. (2)) and the EVPS algorithm.**

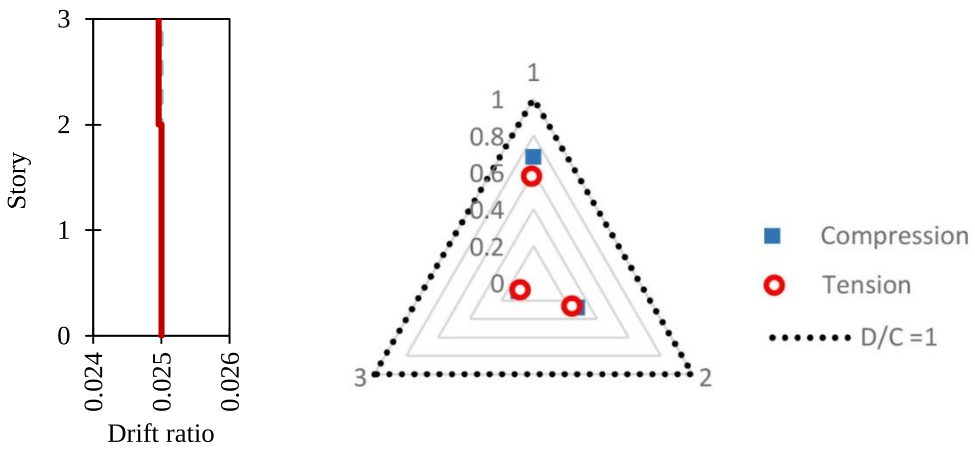


*(a)* Inter story drifts *(b)* Stress ratios

Figure 5. Stress ratios and drift ratios diagrams of the first problem

### *5.2 One-bay six-story frame*

The second problem is the one-bay six-story frame with BRB that is shown in Fig. 2.b. The variation of the *f* (Eq. (2)) against the iteration of the EVPS algorithm for the best answer is illustrated in Fig. 6. Also, this figure shows the trend of decreasing the normalized weight of the structure and increasing normalized energy dissipation for the best solution. Fig. 7 presents the hysteresis curve shows the decrease in base shear (kN) after 5, 55 and 300 iterations which confirms the validity of the optimization.

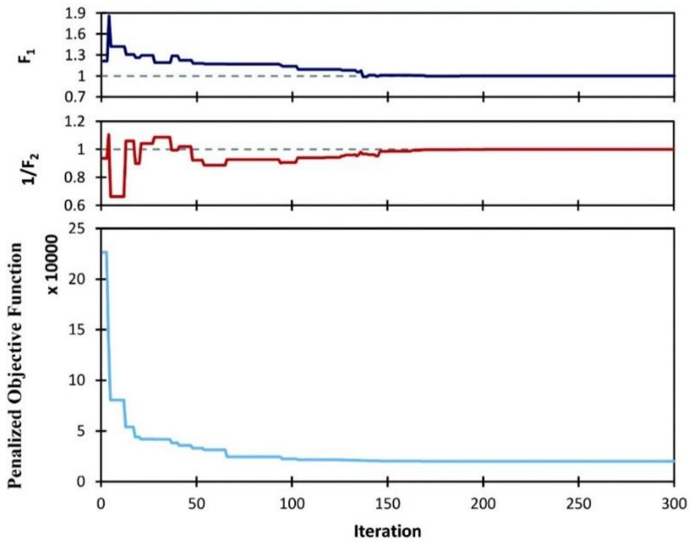


Figure 6. Convergence curve of optimal design of one-bay six-story frame

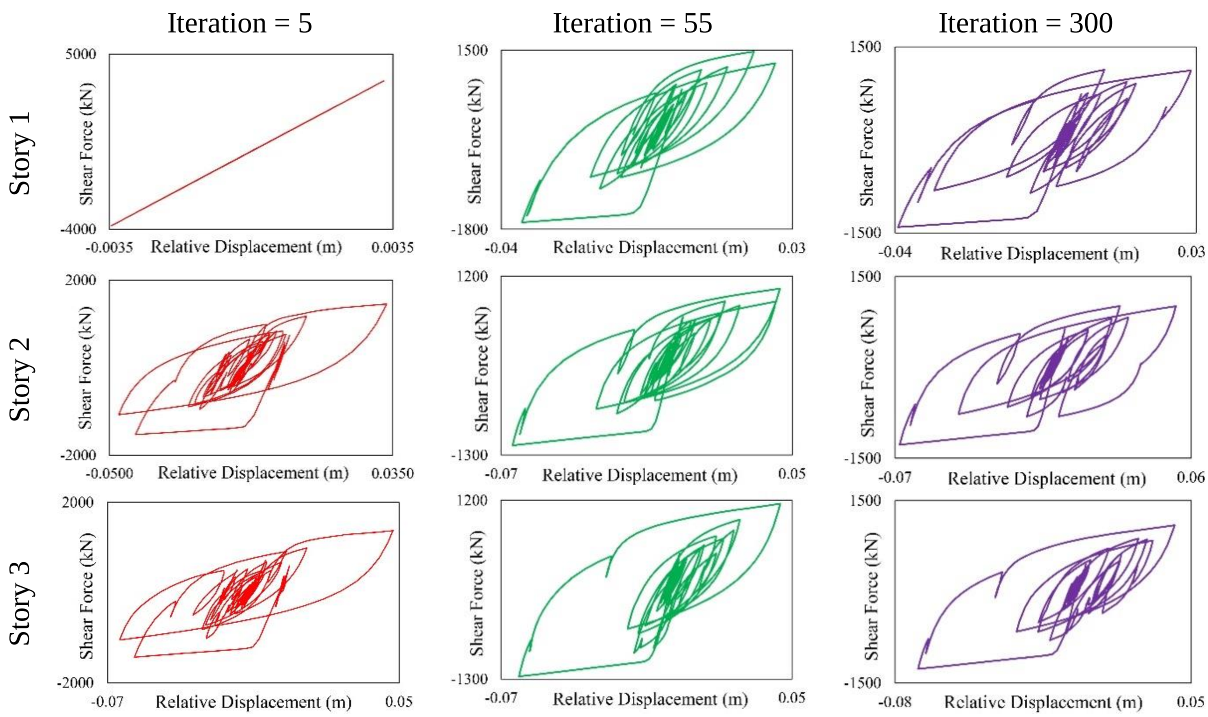

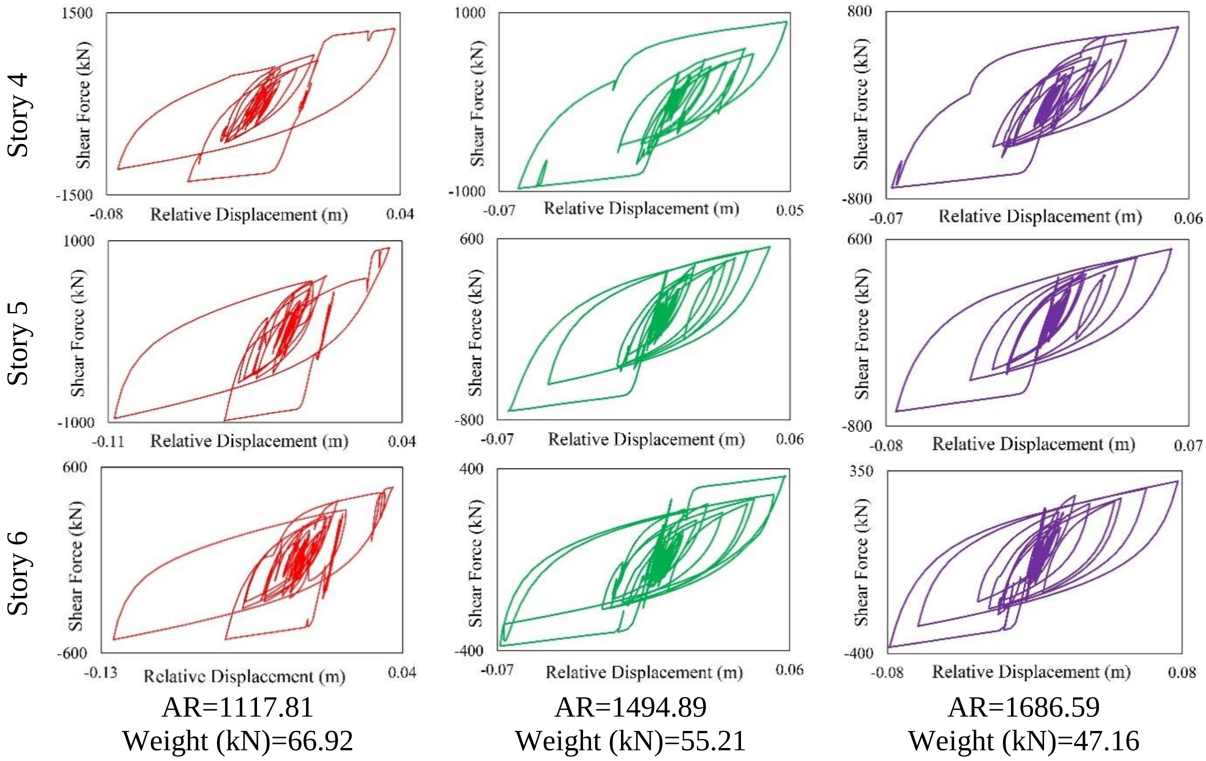


Figure 7. The hysteresis curve after 5, 55 and 300 iterations for the one-bay six-story frame

The optimal sections and the weight of the structures for the best answer gained by EVPS is presented in Table 3. Finally, satisfying the stress ratio of elements and drift of each story are illustrated in Fig. 8.

Table 3: Properties of optimal sections for sample 2

| Element group | LA01 | | | LA12 | | | LA16 | | | LA14 |
|---|---|---|---|---|---|---|---|---|---|---|
| | **ECBO[37]** | **SSA[37]** | **EVPS*** | **ECBO[37]** | **SSA[37]** | **EVPS*** | **ECBO[37]** | **SSA[37]** | **EVPS*** | **EVPS*** |
| **1** | W44×262 | W44×335 | w30X132 | W40×392 | W14×550 | w30X132 | W40×324 | W36×395 | w24X76 | W30×357 |
| **2** | W40×215 | W44×335 | w36X194 | W40×278 | W16×100 | w36X800 | W40×199 | W33×291 | w27X114 | W36×800 |
| **3** | W40×167 | W40×372 | w44X262 | W40×297 | W14×48 | w40X324 | W36×135 | W33×291 | w27X114 | W36×232 |
| **4** | W33×201 | W40×235 | w33X169 | W40×235 | W10×54 | w14X730 | W33×263 | W33×291 | w14X109 | W18×119 |
| **5** | W30×391 | W33×241 | w40X264 | W30×326 | W8×58 | w36X256 | W33×169 | W12×252 | w14X61 | W24×229 |
| **6** | W30×391 | W24×279 | w40X264 | W24×250 | W8×40 | w33X169 | W10×68 | W10×54 | w40X593 | W14×257 |
| **Columns weight (*kN*)** | 82.204 | 135.38 | 37.45 | 127.66 | 105.53 | 36.191 | 90.628 | 130.72 | 68.082 | 38.48 |
| **7**($mm^2$) | 10170 | 13894 | 5218.867 | 16300 | 19317 | 7178.674 | 7353 | 17912 | 5986.983 | 3350 |
| **8**($mm^2$) | 9680 | 8121 | 3328.374 | 1677 | 17872 | 3767.786 | 6942 | 16403 | 5954.923 | 2783 |
| **9**($mm^2$) | 9159 | 7725 | 2124.683 | 645 | 2007 | 912.1746 | 6668 | 12179 | 5721.294 | 2760 |
| **10**($mm^2$) | 5051 | 5688 | 1844.426 | 500 | 1200 | 876.1455 | 6180 | 8001 | 5443.881 | 1553 |
| **11**($mm^2$) | 940 | 1950 | 1839.219 | 500 | 580 | 564.8092 | 5244 | 4486 | 4110.228 | 1477 |
| **12**($mm^2$) | 751.2 | 1318 | 656.0814 | 500 | 500 | 501.4227 | 2175 | 3112 | 1817.46 | 792 |
| **BRB weight (*kN*)** | 24.505 | 26.858 | 10.4 | 15.060 | 29.313 | 9.8 | 23.389 | 42.553 | 19.63 | 8.68 |
| **Total weight (*kN*)** | 106.709 | 162.24 | 47.84909 | 142.719 | 134.842 | 46.03363 | 114.017 | 173.277 | 87.70827 | 47.16 |
| **AR** | 1420.4 | 1053.1 | 2334.93 | 1423.5 | 1070.5 | 1775.75 | 607.2 | 417.7 | 1040.586 | 1686.59 |

*** The marked items are obtained using the new objective function (Eq. (2)) and the EVPS algorithm.**

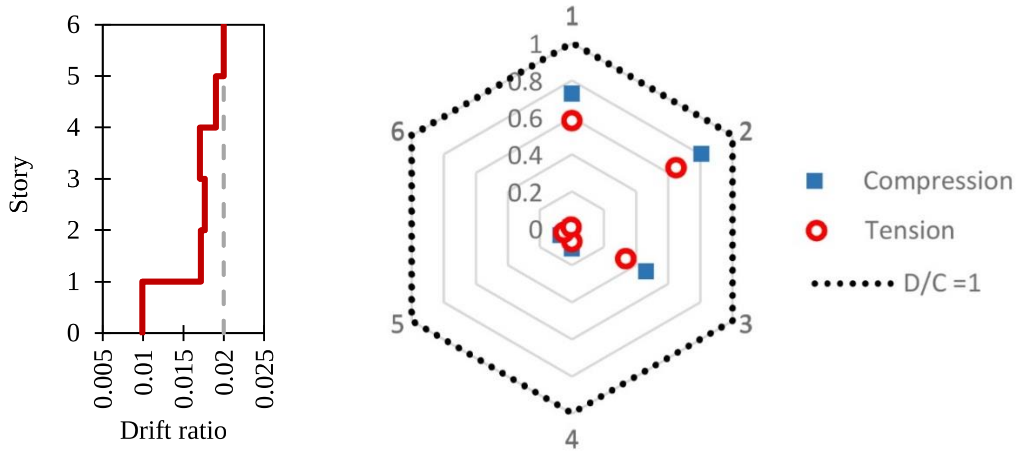


(a) Inter story drifts (b) Stress ratios

Figure 8. Stress ratios and drift ratios diagrams of the one-bay six-story problem

### *5.3 One-bay nine-story frame*

The last problem is the one-bay nine-story frame with BRB that is shown in Fig. 2.c. The variation of the *f* (Eq. (2)) against the iteration of the EVPS algorithm for the best answer is illustrated in Fig. 9. Also, this figure shows the trend of decreasing the normalized weight of the structure and increasing normalized energy dissipation for the best solution.

The optimal sections and the weight of the structures for the best answer gained by the EVPS and ECBO algorithms are presented in Table 4. Finally, satisfying the stress ratio of elements and drift of each story of both algorithms are illustrated in Fig. 10.

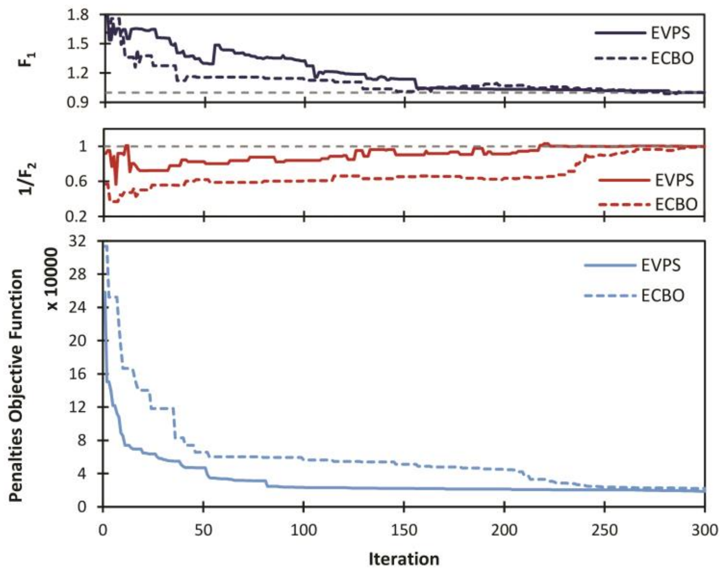


Figure 9. Convergence curve of optimal design of one-bay nine-story frame for the EVPS and ECBO algorithms

Table 4: Properties of optimal sections for sample 3

| **Element group** | **LA14** | |
|---|---|---|
| | **ECBO*** | **EVPS*** |
| **1** | W21X93 | W27X114 |
| **2** | W24X279 | W30X211 |
| **3** | W18X283 | W33X201 |
| **4** | W27X102 | W33X318 |
| **5** | W33X318 | W33X318 |
| **6** | W21X111 | W27X102 |
| **7** | W30X173 | W21X83 |
| **8** | W30X326 | W21X83 |
| **9** | W27X336 | W18X175 |
| **Columns weight (*kN*)** | 106.2 | 70.182 |
| **10**($mm^2$) | 7801.445 | 4089.883 |
| **11**($mm^2$) | 4891.928 | 3609.866 |
| **12**($mm^2$) | 4582.412 | 3086.66 |
| **13**($mm^2$) | 3262.412 | 3086.441 |
| **14**($mm^2$) | 2778.419 | 2940.541 |
| **15**($mm^2$) | 2207.584 | 2690.173 |
| **16**($mm^2$) | 2114.479 | 1952.423 |
| **17**($mm^2$) | 2052.164 | 673.1032 |
| **18**($mm^2$) | 513.1105 | 500.6738 |
| **BRB weight (*kN*)** | 20.6 | 15.23 |
| **Total weight (*kN*)** | 126.764 | 85.41027 |
| **AR** | 1718.2 | 1681.36 |

*** The marked items are obtained using the new objective function (Eq. (2)) and the EVPS algorithm**

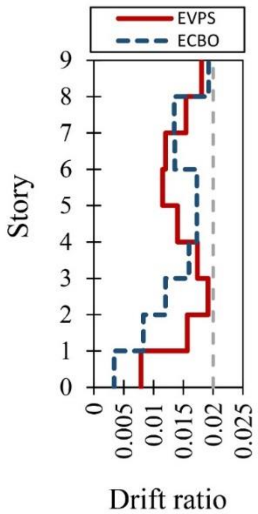


(a) Inter story drifts

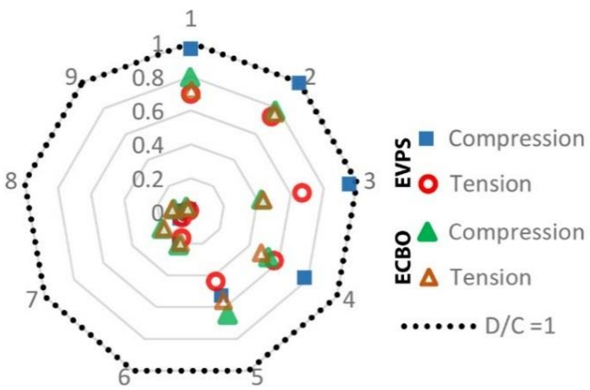


(b) Stress ratios

Figure 10. Stress ratios and drift ratios diagrams of the one-bay nine-story problem

## 6. CONCLUSIONS

In this research, the design of the BRB, according to the defined constraints using the EVPS algorithm and nonlinear time history analysis is investigated. A function that expresses the weight and amount of energy dissipation of structure is considered as the objective function. By minimizing the objective function, the two objectives are satisfied, the first of which is the weight of the structure which is to be minimized and the second one is the energy dissipation which is to be maximized. According to the presented results, the proposed objective function fulfills the desired goal (the results show the trend of decreasing in normalized weight of the structure and the shear base also increasing in normalized energy dissipation). The EVPS optimization algorithm has already been investigated in various optimization problems and has obtained acceptable results. Based on the results, this algorithm can obtain an acceptable solution for these types of problems. The results show that the BRB weight has less effect on the overall weight of the structure and the columns have the most influence on the structural weight; instead, the BRB elements reduce the base shear and thus reduce the weight of the structure.

## REFERENCES


1. Kaveh A. *Advances in Metaheuristic Algorithms for Optimal Design of Structures*, Springer, 2014.
2. Kaveh A. *Applications of Metaheuristic Optimization Algorithms in Civil Engineering*, Springer, 2017.
3. Csébfalvi A, Lógó J. A critical analysis of expected-compliance model in volume-constrained robust topology optimization with normally distributed loading directions, using a minimax-compliance approach alternatively, *Adv Eng Softw* 2018; **120**: 107-15.
4. Kaveh A, Hoseini Vaez SR, Hosseini P. Simplified dolphin echolocation algorithm for optimum design of frame, *Smart Struct Syst* 2018; **21**: 321-33.
5. Kaveh A, Hoseini Vaez SR, Hosseini P, Ezzati E. Layout optimization of planar braced frames using modified dolphin monitoring operator, *Period Polytech Civil Eng* 2018; **62**(3): 717-31.
6. Pastore T, Mercuri V, Menna C, Asprone D, Festa P, Auricchio F. Topology optimization of stress-constrained structural elements using risk-factor approach, *Comput Struct* 2019; **224**: 106104.
7. Tian Y, Pu Sh, Zong Z, Shi T, Xia Q. Optimization of variable stiffness laminates with gap-overlap and curvature constraints, *Compos Struct* 2019; **230**: 111494.
8. Kaveh A, Hoseini Vaez SR, Hosseini P, Bakhtyari M. Optimal design of steel curved roof frames by enhanced vibrating particles system algorithm, *Period Polytech Civil Eng* 2019; **63**(4): 947-60.
9. Storn R, Price K. Differential evolution–a simple and efficient heuristic for global optimization over continuous spaces, *J Global Optim* 1997; **11**(4): 341-59.
10. Eberhart R, Kennedy J. A new optimizer using particle swarm theory, in *MHS'95. Proceedings of the Sixth International Symposium on Micro Machine and Human Science*, IEEE, 1995.

11. Kaveh A, Ilchi Ghazaan M. A comparative study of CBO and ECBO for optimal design of skeletal structures, *Comput Struct* 2015; **153**: 137-47.
12. Beşkirli M, et al. A new optimization algorithm for solving wind turbine placement problem: Binary artificial algae algorithm, *Renewab Ener* 2018; **121**: 301-8.
13. Tabari A, Ahmad A. A new optimization method: Electro-Search algorithm, *Comput Chemic Eng* 2017; **103**: 1-11.
14. Kaveh A, Dadras A. A novel meta-heuristic optimization algorithm: Thermal exchange optimization, *Adv Eng Softw* 2017; **110**: 69-84.
15. Trivedi IN, et al. *A Novel Hybrid PSO–WOA Algorithm for Global Numerical Functions Optimization*, Singapore, Springer Singapore, 2018.
16. Kaveh A, Hoseini Vaez SR, Hosseini P. Enhanced vibrating particles system algorithm for damage identification of truss structures, *Sci Iran* 2019; **26**(1): 246-56.
17. Kaveh A, Hoseini Vaez SR, Hosseini P. MATLAB code for an Enhanced Vibrating Particles System Algorithm, *Int J Optim Civil Eng* 2018; **8**(3): 401-14.
18. Balling RJ, Balling LJ, Richards PW. Design of buckling-restrained braced frames using nonlinear time history analysis and optimization, *J Struct Eng* 2009; **135**(5): 461-8.
19. Chopra AK, McKenna F. Modeling viscous damping in nonlinear response history analysis of buildings for earthquake excitation, *Earthq Eng Struct Dyn* 2016; **45**(2): 193-211.
20. Gong Y, et al. Energy-based design optimization of steel building frameworks using nonlinear response history analysis, *J Construct Steel Res* 2012; **68**(1): 43-50.
21. He Z, et al. New speedup algorithms for nonlinear dynamic time history analysis of supertall building structures under strong earthquakes, *Struct Des Tall Special Build* 2017; **26**(16): e1369.
22. Hoffman EW, Richards PW. Efficiently implementing genetic optimization with nonlinear response history analysis of taller buildings, *J Struct Eng* 2014; **140**(8): A4014011.
23. Jaradat O, Lai C, Elsadek A. *Crane-Wharf Interaction Nonlinear Time-History Analysis for Pier E Wharf at the Port of Long Beach*, in *Ports 2013: Success through Diversification*, 2013; 1255-64.
24. Kim NH, Choi KK. Design sensitivity analysis and optimization of nonlinear transient dynamics, *Mech Struct Mach* 2001; **29**(3): 351-71.
25. Lu X, et al. A shear wall element for nonlinear seismic analysis of super-tall buildings using OpenSees, *Finite Elemen Anal Des* 2015; **98**: 14-25.
26. Pant DR, Wijeyewickrema AC, ElGawady MA. Appropriate viscous damping for nonlinear time-history analysis of base-isolated reinforced concrete buildings, *Earthq Eng Struct Dyn* 2013; **42**(15): 2321-39.
27. Hosseinzadeh S, Mohebi B. Seismic evaluation of all-steel buckling restrained braces using finite element analysis, *J Construct Steel Res* 2016; **119**: 76-84.
28. Dong H, et al. Performance of an innovative self-centering buckling restrained brace for mitigating seismic responses of bridge structures with double-column piers, *Eng Struct* 2017; **148**: 47-62.
29. Sabelli R, Mahin S, Chang C. Seismic demands on steel braced frame buildings with buckling-restrained braces, *Eng Struct* 2003; **25**(5): 655-66.

30. Kiggins S, Uang CM. Reducing residual drift of buckling-restrained braced frames as a dual system, *Eng Struct* 2006; **28**(11): 1525-32.
31. Kim J, Choi H. Behavior and design of structures with buckling-restrained braces, *Eng Struct* 2004; **26**(6): 693-706.
32. Sahoo DR, Chao SH. Performance-based plastic design method for buckling-restrained braced frames, *Eng Struct* 2010; **32**(9): 2950-8.
33. Miller DJ, Fahnestock LA, Eatherton MR. Development and experimental validation of a nickel–titanium shape memory alloy self-centering buckling-restrained brace, *Eng Struct* 2012; **40**: 288-98.
34. Hoveidae N, Rafezy B. Overall buckling behavior of all-steel buckling restrained braces, *J Construct Steel Res* 2012; **79**: 151-8.
35. Fahnestock LA, Ricles JM, Sause R. Experimental evaluation of a large-scale buckling-restrained braced frame, *J Struct Eng* 2007; **133**(9): 1205-14.
36. Fahnestock LA, Sause R, Ricles JM. Seismic response and performance of buckling-restrained braced frames, *J Struct Eng* 2007; **133**(9): 1195-204.
37. Abedini H, Hoseini Vaez SR, Zarrineghbal A. Optimum design of buckling-restrained braced frames, *Struct* 2020; **25**: 99-112.
38. Kersting RA, Fahnestock LA, López WA. Seismic design of steel buckling-restrained braced frames, *NIST GCR* 2015: 15-917.
39. Somerville PG. *Development of Ground Motion Time Histories for Phase 2 of the FEMA/SAC Steel Project*, SAC Joint Venture, 1997.
40. Mazzoni S, et al. OpenSees Command Language Manual, Pacific Earthquake Engineering Research (PEER) Center, 2006; **264**.
41. Specification for structural steel buildings (ANSI/AISC 360-10), *American Institute of Steel Construction, Chicago-Illinois*, 2010.
42. Zou XK, Chan CM. Optimal seismic performance-based design of reinforced concrete buildings using nonlinear pushover analysis, *Eng Struct* 2005; **27**(8): 1289-302.
43. ASCE A. *Minimum Design Loads for Buildings and other Structures*, Reston, VA, 2010.
44. AISC, *341(2010) Seismic Provisions for Structural Steel Buildings*, American Institute of Steel Construction, Chicago, 2010.
45. Kaveh A, Shakouri Mahmud Abadi, A. Cost optimization of composite floor system using an improved harmony search algorithm, *J Construct Steel Res* 2010; **66**: 664-9.
46. Kaveh A, Hoseini Vaez SH, Hosseini P. Performance of the modified dolphin monitoring operator for weight optimization of skeletal structures, *Period Polytech Civil Eng* 2019; **63**(1): 30-45.